

# Detection of Renal Hypoxia Configuration in Patients with Lupus Nephritis: A Primary Study Using Blood Oxygen Level–Dependent MR Imaging

**Zhengfeng Zheng**

Tianjin Medical University General Hospital

**Yanyan Wang**

Tianjin Medical University General Hospital

**Tiekun Yan**

Tianjin Medical University General Hospital

**Junya Jia**

Tianjin Medical University General Hospital

**Dong Li**

Tianjin Medical University General Hospital

**Li Wei**

Tianjin Medical University General Hospital

**Wenya Shang**

Tianjin Medical University General Hospital

**huilan shi** (✉ [shihuilan@vip.126.com](mailto:shihuilan@vip.126.com))

Tianjin Medical University General Hospital

---

## Research article

**Keywords:** lupus nephritis; blood oxygen level dependent; renal hypoxia; magnetic resonance imaging

**Posted Date:** July 25th, 2019

**DOI:** <https://doi.org/10.21203/rs.2.11872/v1>

**License:**  This work is licensed under a Creative Commons Attribution 4.0 International License.

[Read Full License](#)

---

**Version of Record:** A version of this preprint was published at Abdominal Radiology on October 20th, 2020. See the published version at <https://doi.org/10.1007/s00261-020-02794-y>.

# Abstract

**Background** Renal microstructure and function are closely associated with homeostasis of oxygenation. Analyzing renal blood oxygen level–dependent (BOLD) magnetic resonance imaging (MRI) examination results will provide information on the biological status of the kidneys. The current study was performed to explore the hypoxia mode of the entire renal parenchyma in patients with lupus nephritis (LN).

**Methods** Twenty-three adult patients with LN and eighteen healthy volunteers were recruited.  $R2^*$  values were acquired through the use of the BOLD MRI analysis technique. The narrow rectangular region of interest was used to explore the hypoxia configuration in entire depths of renal parenchyma. Acquired sequential  $R2^*$  data were fitted by using four categories of mathematic functions. The tendency of  $R2^*$  data in both patients with LN and healthy volunteers was also compared through the use of repeated-measures analysis of variance. Results  $R2^*$  data from the superficial cortex to deep medulla displayed two patterns, called a sharp uptrend style and a flat uptrend style. After sequential  $R2^*$  data were fitted individually with the use of four mathematic formulas, the multiple-compartment Gaussian function showed the highest goodness of fit. Compared with two categories of  $R2^*$  value styles, the  $R2^*$  tendency of entire parenchyma in patients with LN was different from that in healthy volunteers.

**Conclusions** Deep renal medullary oxygenation was not always overtly lower than oxygenation in superficial renal cortical zone. Renal parenchyma oxygenation manifestation could be described through the use of a Gaussian function model. The deoxygenation tolerance capability was damaged in patients with LN.

## Background

Lupus nephritis (LN) is the primary cause of secondary glomerulonephritis in patients in China [1]. Renal microstructure and function changes are closely associated with glomerular function and kidney prognosis. Precise evaluation of renal pathophysiological injuries is key in the treatment of patients with LN [2, 3]. Unfortunately, there are no ideal methods of simultaneously detecting renal structure and pathophysiological status. Although renal biopsy specimen examination has been successfully applied in clinical practice for several decades, this technique is not considered to be ideal because of multiple inherent shortcomings, such as serious bleeding complications [4], incommensurable field of view for inspection, and limited biopsy specimen locations. Therefore, a new, noninvasive, comprehensive assessment method is needed.

By using the paramagnetic properties of deoxyhemoglobin, the blood oxygen level–dependent (BOLD) magnetic resonance imaging (MRI) technique was deemed as a promising reliable and noninvasive inspection manner. Since the first renal BOLD MRI study was reported by Prasad in 1996 [5], investigators have increasingly explored renal oxygenation principles and tissue hypoxia mechanisms. During the past two decades, many renal physiological manifestations and formation mechanisms have been elucidated. These well-accepted renal physiological discoveries were corroborated with BOLD MRI results. For example, renal tissue in the medullary zone had a lower oxygen partial pressure and hypoxia gradient than in the entire kidney parenchyma [6]. The corresponding results were obtained from renal BOLD maps analyzed by use of the concentric objects (CO) [7] and twelve-layer concentric objects (TLCO) techniques

[8]. Although substantial valuable discoveries have been reported by nephrologists and radiologists worldwide, several issues have prevented BOLD MRI from extensive clinical use and have frustrated initial research enthusiasm. The first issue concerns the origin of the renal BOLD signals. It is well known that massive physicochemical or biological factors are involved in renal BOLD signal formation. These factors include regional blood oxygen supplementation, tissue oxygen consumption, hydration status, hematocrit, and salt and medicine intake [9-11]. Therefore, analysis of the BOLD signal value alone cannot determine which solitary or multiple factors are the key factors. A second problem relates to the method of renal BOLD signal analysis. Although the acquisition of renal BOLD MR images is easily performed worldwide, there is no consensus as to how to analyze the BOLD MR images. Different analysis methods could lead to significantly different results. For example, Milani et al. investigated the difference in the  $R2^*$  value between patients and control subjects and did not find any difference in  $R2^*$  with the use of the conventional regional ROI technique. However, significant differences in  $R2^*$  values in cortical layers were revealed when the TLCO technique was adopted in the same patient cohort [8]. Overcoming these native deficiencies of BOLD MRI may assist in further understanding renal tissue oxygenation.

The main purposes of this study were to understand renal parenchyma hypoxia configuration and to develop a new BOLD image analysis method. We also compared tissue hypoxia characteristics between healthy people and patients with LN.

## **Methods**

### **Study protocol**

#### **Patients**

A total of forty-one participants including twenty-three patients with LN and eighteen healthy volunteers were accrued from January 2017 to June 2018. After our study protocol were examined by Tianjin Medical University General Hospital Ethical Committee and all participants have signed informed consent files, this study was authorized to carry out. Patients with lupus nephritis were diagnosed by experienced nephrologist according to the 2012 International Collaborating Clinics classification criteria for systemic lupus erythematosus [12]. Renal functional assessment was used estimated glomerular filtration rate (eGFR) by measured serum creatinine according to Chronic Kidney Disease Epidemiology Collaboration (CKD-EPI) equation [13]. Healthy volunteers were recruited from different divisions of our hospital. Since renal oxygenation were mainly affected by oxygen supplementation and consumption, several special conditions should be avoided as much as possible. These conditions included oxygen inhalation, water or salt overload, specific medication such as diuretics, vasodilators or hematopoietin

#### **MRI techniques**

We acquired renal BOLD-MRI images by using a 3.0-T scanner (GE Discovery™ 750 3.0T; General Electric; USA). The detailed imaging parameters can be referred to our previous study [14]

## **Image analysis**

Renal tissue oxygenation distribution was displayed by visualized  $R2^*$  map by processing with FUNCTOOL program. Renal coronal anatomical plane with largest area was selected as analyzed section. The region of interest (ROI) was set as a 1 pixel (width) × 50 pixels (height) rectangle. One tip of the ROI was located on the renal cortical surface. Another tip of the ROI looked out on the renal hilus (Figure 1).  $R2^*$  values of each voxel of the selected ROI were obtained with MATLAB 2014a (MathWorks Inc., Natick, MA, USA).

## **Statistical analyses**

### **RM-ANOVA data**

$R2^*$  values of renal BOLD maps were expressed as mean standard deviation (SD). To compare the  $R2^*$  level difference between the group with LN and the control group at different depths of renal parenchyma, repeated-measures analysis of variance (RM-ANOVA) was performed. Mauchly's test was used to check whether the covariance structure satisfied the sphericity condition [15]. If the covariance matrix was satisfied with sphericity assumption, the univariate RM-ANOVA was applied for further analysis. Otherwise, multivariate ANOVA was used to analyze the data [16], and four multivariate test statistics were also calculated: Pillai's Trace statistic, Wilks' likelihood ratio, the Hotelling-Lawley Trace criterion, and Roy's Largest Root. The effects of intergroup (LN vs healthy control) and intragroup (different depths of renal parenchyma) were compared. The interaction effect was also compared. Statistical significance was accepted at  $P < 0.05$ . All analyses were carried out using the IBM® SPSS® Statistics software (version 22.0.0.0 IBM Corporation, Armonk, NY, USA).

### **Curve-fitting analysis**

To describe the  $R2^*$  configuration throughout the cortex and medulla, the curve-fitting analysis was selected to explore the detected  $R2^*$  data. Four curve fit types (polynomial, power, exponential, and Gaussian) were chosen for data exploration. The goodness of fit was assessed with the use of multiple parameters including  $R^2$ , sum square error (ESS), and root-mean-square error (RMSE). All analyses were carried out by using the Curve Fitting Toolbox of MATLAB R2014a (MathWorks Inc.).

## **Results**

## **Manifestation of R2\* values in renal parenchyma from superficial cortex to deep medulla**

According to the detection results from the rectangular ROI of BOLD MRI, we found at least two pattern categories of R2\* manifestation in the renal parenchyma. The first R2\* pattern in the renal parenchyma displayed two different styles, shown in the cortex and the medulla. In the cortex or cortical–medullary conjunction zone, the increment of R2\* values concomitant with increasing depth renal parenchyma was slight, fluctuating in a small range. However, a conspicuous uptrend of R2\* values was observed in the deeper medulla zone. Compared with the correlation between R2\* values and renal depth of parenchyma, the slope of R2\* values in the deeper medulla zone was steeper than that in the cortex zone. We call this pattern of R2\* values the “sharp uptrend style.” The second R2\* pattern in kidneys was different from the first pattern. The R2\* values maintained a relatively stable level throughout the cortical and medullary zones. We call this pattern of R2\* values the “flat uptrend style” (Figure 2).

## **Analysis of two patterns of R2\* values shows a difference between patients with LN and healthy volunteers**

To study the sharp uptrend style pattern of R2\* data, we selected eight samples that had the maximum average and range among the whole sample of data for each subject. Because the height of the rectangular ROI was 50 pixels, we divided the renal parenchyma into 50 layers. The average R2\* values in each renal parenchyma layers are shown in Figure 3.

There was a very small difference in the R2 value curves between the LN group and the control group when the depth of renal parenchyma was less than 25 layers. However, the slope of the R2\* curve in the LN group was lower than that in the control group at a depth of 25-50 renal layers. We compared the sharp uptrend style pattern of R2\* values in both the LN group and the control group by using RM-ANOVA. Because Mauchly's test showed that covariance structure was not satisfied with sphericity assumption ( $P < 0.001$ ), multivariate ANOVA was chosen for further data. The statistical difference in R2\* values between renal parenchyma layers was observed in both the LN group and the healthy volunteer group (Pillai's Trace statistic,  $P < 0.001$ ; Wilks' likelihood ratio,  $P < 0.001$ ; Hotelling-Lawley Trace criterion,  $P < 0.001$ ; Roy's Largest Root,  $P < 0.001$ ). The statistical interaction effect between renal parenchyma layers and study groups was also observed (Pillai's Trace statistic,  $P = 0.004$ ; Wilks' likelihood ratio,  $P = 0.004$ ; Hotelling-Lawley Trace criterion,  $P = 0.004$ ; Roy's Largest Root,  $P = 0.004$ ).

Similar results were found for the flat uptrend style pattern of R2\* data. In the superficial zone of renal parenchyma (less than 25 layers), the location of the R2\* curve in the LN group was lower than that in the control group. However, the difference in R2\* values in the deep medullary zone was not distinct. RM-ANOVA results showed a statistic difference between the two R2\* curves. Multivariate ANOVA was used again because of the similar Mauchly's test results. Both difference in renal parenchyma layers and interaction effect with study groups showed statistical significance (Pillai's Trace statistic,  $P < 0.001$ ;

Wilks' likelihood ratio,  $P < 0.001$ ; Hotelling-Lawley Trace criterion,  $P < 0.001$ ; Roy's Largest Root,  $P < 0.001$ ) (see Figure 3).

### **Comparison of R2\* data goodness of fit by multiple mathematic function models**

We collected several sets of R2\* data from the renal parenchyma in both patients with LN and healthy volunteers. Four categories of mathematic functions (polynomial, power, exponential, and Gaussian functions) were used to fit virtual R2\* data. By comparison with goodness of fit indexes, the Gaussian functional model was recognized as the best-fit model for both sharp uptrend style data or flat uptrend style data. Goodness of fit indexes for the four mathematic functional models are listed in Tables 1 and 2. The fit curves of these models are displayed in Figure 4.

## **Discussion**

One of the primary aims was to understand the relationship between tissue oxygenation and renal parenchyma depth. Our current study revealed two categories of renal oxygenation manifestation patterns. One pattern, the sharp uptrend style, has better tissue oxygenation with a slight fluctuation in the superficial layers of the kidney. Subsequently, a sharp increment of deoxygenation was observed in the deep layers of the renal parenchyma. Although this pattern has similar characteristics with the well-known renal tissue oxygenation feature, such as higher deoxygenation in the medulla than in the cortex [17], a distinct two-phase oxygenation feature was different from that in many previous studies [18-20]. This sharp uptrend style of renal R2\* values might correlate with a sophisticated relationship between tissue partial pressure of oxygen ( $\text{PaO}_2$ ) and oxyhemoglobin saturation dissociation curve. Tissue oxyhemoglobin saturation could be maintained in a stabilized level when  $\text{PaO}_2$  is above 60 mmHg, whereas there is a steep gradient with a sharp decrease in oxyhemoglobin when the  $\text{PaO}_2$  is less than 26.6 mmHg. Previous research has shown that  $\text{PaO}_2$  in the majority of cortexes is usually higher than 60 mmHg, whereas medullary  $\text{PaO}_2$  rarely exceeds 26.6 mmHg [21].

Another relevant reason was interrelated with 2,3-diphosphoglycerate (DPG)-mediated oxyhemoglobin affinity. A lessening in oxyhemoglobin affinity has been deemed as an important physiological adaptive response to conditions in which oxygen delivery is impaired. The increased oxyhemoglobin affinity may actually impair tissue oxygenation [22]. Moreover, another pattern of R2\* values, the flat uptrend style, was also found in our current study. We found that the R2\* values fluctuated in a narrow range throughout the depth of renal parenchyma. R2\* values in the deep medulla were only slightly higher than those in the superficial cortex. We even found no discrepancy in R2\* level between the superficial renal zone and the deep renal zone, in sporadic samples. This phenomenon implies that tissue oxygenation in the deep medullary zone is not always lower than that in the superficial cortical zone. This discovery is a challenge to the recognized opinion that had been testified by many studies.

The reason why previous studies did not find this exception may derive from the ROI mode, which could remarkably affect the detective  $R2^*$  value. For example, the TLCO technique was recognized as the preferable manner by which renal  $R2^*$  values were measured in the past few years [8]. The entire renal parenchyma of the  $R2$  map image was divided into 12 consecutive equivalent depths of the zone. Subsequently, the  $R2^*$  value of each pixel was detected, and the average  $R2^*$  value in each zone was also calculated. Because of lower variability and higher stability in repeated measures, this renal  $R2^*$  acquired technique was well accepted by many investigators. However, the calculated average  $R2^*$  value was usually prone to affect by higher medullary  $R2^*$  data instead of those lower  $R2^*$  data. Under this circumstance, the phenomenon of lower  $R2^*$  level in the deep medulla was concealed by this technique. There was no plausible explanation for this new discovery as observed in our study. We thought that the microstructure and physiological status in that deep medulla zone might discriminate those renal medullary tissues where the typical oxygenation pattern was easily observed.

Another result of our study involved exploring the possibility of describing renal parenchyma  $R2^*$  patterns by mathematic models. Some investigators thought that the renal tissue oxygenation status was influenced by multiple factors, such as local blood supplementation and tissue oxygen consumption. Therefore, detected  $R2^*$  values in each pixel from anywhere in the BOLD images were always the integrated results of multiple physiological factors. The key problem was that the precise participation proportion of each factor was not well understood. However, we believed that information on all involved physiological factors with similar to the encrypted message was still sealed in these  $R2^*$  maps. We still hope to unlock this sealed information with the right decoding method. By testing the multiple mathematic functions, we found that Gaussian function had the best capability to fit practical  $R2^*$  data. Moreover, both the sharp uptrend style data and the flat uptrend style data fit the Gaussian function well with two or more compartments. Although there was no reliable evidence to verify the corresponding relationship between renal biological factors and compartments of fit Gaussian functions, we hypothesized that those multiple encrypted and perplexing physiological messages in the  $R2^*$  data could be transformed into another mode. Perhaps we will decode the encrypted biological messages that were composed in  $R2^*$  data by studying fit Gaussian functions.

In our current study, we also investigated the oxygenation discrepancy between patients with LN and healthy volunteers. Instead of measuring average  $R2^*$  values in the renal parenchyma, we focused on the extreme  $R2^*$  data in both the LN group and the control group. In each study subject, two categories of extreme data were also selected. One had the highest average with the maximal range, and the other had the lowest mean value with the minimal range. We thought these two categories of data stood for the tolerant capacity in tissue deoxygenation and preserved capability in tissue oxygenation. Our study revealed that the tolerant capacity in renal tissue deoxygenation was damaged in the patients with LN. The  $R2^*$  values of the deep medullary zone in the patients with LN were slightly lower than those in healthy volunteers. In contrast, the preserved capability in tissue oxygenation was also spoiled in the patients with LN. The  $R2^*$  values of the superficial cortical zone in the patients with LN were also slightly lower than those in healthy volunteers. One possible explanation was that renal tissue deoxygenation in the medulla primarily derived from oxygen consumption in tubular transport proteins. If these transport

proteins were diminished or disabled under pathological circumstances, the oxygen consumption also decreased, and that was why the lower  $R2^*$  values could be observed in the kidneys of the patients with LN. A previous study conducted by our team showed similar results.

In proliferative LN such as type III or type IV, lower renal tissue  $R2^*$  values usually correspond with severe tubular damage. The inverse manifestation was observed in nonproliferative LN in which mild tubular injuries could be confirmed with renal biopsy samples [23]. Despite statistical discrepancy of  $R2^*$  values detected between the two groups in both sharp uptrend and flat uptrend style data, the substantial  $R2^*$  difference was very small. We speculated that at least two factors were involved and that the native mechanism was similar to that in patients with renal artery stenosis. Hansell et al. found that kidneys usually had increased renal blood flow instead of local  $PO_2$  when the renal parenchyma was under severe hypoxia conditions. The increased renal blood flow also led to glomerular filtration rate increments that subsequently induced more filtered sodium in the renal tubules. The reinforced tubular sodium reabsorption was the main reason for increased oxygen consumption [24].

We also developed a novel ROI method called the “narrow rectangle” or “virtual probe” to measure renal  $R2^*$  values. This was the principal reason why we devised and applied this special ROI technique. Renal microstructure displays distinct directional characteristics and spatial heterogeneity. Renal parenchyma oxygenation features are based on its histological anatomy foundation. The well-known opinion that the degree of renal blood oxygen saturation in the cortical zone is always higher than that in the medullary zone is based on previous ROI analysis methods such as regional ROI selection [25], compartmental approach [26], fractional kidney hypoxia [27], CO [7], and TLCO [8]. However, investigators either handled nonconsecutive crude  $R2^*$  data by regional ROI selection or acquired calculated mean  $R2^*$  results by CO and TLCO methods. These inherent shortcomings remained an obstacle to the procurement of the explicit oxygenation tendency throughout the renal parenchyma. Contrary to previous conventional ROI analysis methods, our new analysis technique revealed that deep medullary oxygenation was not always overtly lower than cortical oxygenation. This unusual discovery challenged the well-known opinion.

Our current study still had several shortcomings. First, our study merely investigated renal  $R2^*$  signal instead of other functional MR signals such as ADC, synchronously. We only knew the existing oxygenation condition, whereas we did not understand the precise mechanism of hypoxia status formation. Second, the meaning of fitted Gaussian functions had not yet been explained or proved by other physiological studies, and we only hypothesized that fitted Gaussian formulas represent renal hypoxia outline in the kidney cortical and medullary zones. Third, the narrow rectangular ROI analysis method that was adopted in our study had not been tested by many researchers. Because the highly observer-dependent property of previous conventional ROI analysis methods has been proved, we did not know the new ROI analysis technique had the highly reproducible and lower variant characteristic.

## Conclusions

Deep renal medullary oxygenation was not always overtly lower than that in the superficial renal cortical zone. Renal parenchyma oxygenation manifestation could be described by the Gaussian function model. The deoxygenation tolerance capability was damaged in patients with LN.

## Abbreviations

Blood oxygen level dependent, **BOLD**; Chronic Kidney Disease Epidemiology Collaboration ,**CKD-EPI**; Concentric objects, **CO**; Field of view, **FOV**; Functional magnetic resonance imaging, **fMRI**; Lupus nephritis, **LN**; Magnetic resonance imaging, **MRI**; Region of interest, **ROI**; Repeated-measures analysis of variance, **RM-ANOVA**; Root-mean-square error, **RMSE**; Systemic lupus erythematosus, **SLE**; SLE Disease Activity Index, **SLEDAI**; Spoiled gradient recalled echo, **SPGR**; Sum square error, **ESS**; Twelve-layer concentric objects, **TLCO**; Repetition time, **TR**; Echo time, **TE**;

## Declarations

### Ethics approval and consent to participate

This study was approved by the ethics committee of Tianjin Medical University General Hospital prior to the commencement of the study. Written informed consent for participation was obtained from the patient or a legal representative.

### Consent for publication

Not applicable

### Availability of data and material

The datasets used and/or analyzed during the current study are available from the corresponding author on reasonable request.

### Competing interests

The authors declare that they have no competing interests.

### Funding

No funding

## Authors' contributions

ZFZ and YYW are the guarantors of integrity of the entire study and are also responsible for study concepts and design. HLS and TKY are in charge of MR imaging, data analysis and manuscript drafting. JYJ and DL are responsible for renal clinical data. LW and WYS are responsible for renal biopsy and pathological diagnosis. We confirm that all the listed authors have participated actively in the study, and have seen and approved the submitted manuscript.

## Acknowledgements

We thank LetPub ([www.letpub.com](http://www.letpub.com)) for its linguistic assistance during the preparation of this manuscript.

## References

1. Pan Q, Li Y, Ye L, Deng Z, Li L, Feng Y, Liu W, Liu H: **Geographical distribution, a risk factor for the incidence of lupus nephritis in China.** *BMC nephrology* 2014, **15**:67.
2. Austin HA, 3rd, Boumpas DT, Vaughan EM, Balow JE: **Predicting renal outcomes in severe lupus nephritis: contributions of clinical and histologic data.** *Kidney international* 1994, **45**(2):544-550.
3. Bihl GR, Petri M, Fine DM: **Kidney biopsy in lupus nephritis: look before you leap.** *Nephrology, dialysis, transplantation : official publication of the European Dialysis and Transplant Association - European Renal Association* 2006, **21**(7):1749-1752.
4. Corapi KM, Chen JL, Balk EM, Gordon CE: **Bleeding complications of native kidney biopsy: a systematic review and meta-analysis.** *American journal of kidney diseases : the official journal of the National Kidney Foundation* 2012, **60**(1):62-73.
5. Prasad PV, Edelman RR, Epstein FH: **Noninvasive evaluation of intrarenal oxygenation with BOLD MRI.** *Circulation* 1996, **94**(12):3271-3275.
6. Pallone TL, Robertson CR, Jamison RL: **Renal medullary microcirculation.** *Physiological reviews* 1990, **70**(3):885-920.
7. Piskunowicz M, Hofmann L, Zuercher E, Bassi I, Milani B, Stuber M, Narkiewicz K, Vogt B, Burnier M, Pruijm M: **A new technique with high reproducibility to estimate renal oxygenation using BOLD-MRI in chronic kidney disease.** *Magnetic resonance imaging* 2015, **33**(3):253-261.
8. Milani B, Ansaloni A, Sousa-Guimaraes S, Vakilzadeh N, Piskunowicz M, Vogt B, Stuber M, Burnier M, Pruijm M: **Reduction of cortical oxygenation in chronic kidney disease: evidence obtained with a new analysis method of blood oxygenation level-dependent magnetic resonance imaging.** *Nephrology, dialysis, transplantation : official publication of the European Dialysis and Transplant Association - European Renal Association* 2017, **32**(12):2097-2105.

9. Prasad PV, Epstein FH: **Changes in renal medullary pO<sub>2</sub> during water diuresis as evaluated by blood oxygenation level-dependent magnetic resonance imaging: effects of aging and cyclooxygenase inhibition.** *Kidney international* 1999, **55**(1):294-298.
10. Pruijm M, Hofmann L, Maillard M, Tremblay S, Glatz N, Wuerzner G, Burnier M, Vogt B: **Effect of sodium loading/depletion on renal oxygenation in young normotensive and hypertensive men.** *Hypertension (Dallas, Tex : 1979)* 2010, **55**(5):1116-1122.
11. Neugarten J: **Renal BOLD-MRI and assessment for renal hypoxia.** *Kidney international* 2012, **81**(7):613-614.
12. Petri M, Orbai AM, Alarcon GS, Gordon C, Merrill JT, Fortin PR, Bruce IN, Isenberg D, Wallace DJ, Nived O *et al*: **Derivation and validation of the Systemic Lupus International Collaborating Clinics classification criteria for systemic lupus erythematosus.** *Arthritis and rheumatism* 2012, **64**(8):2677-2686.
13. Levey AS, Stevens LA, Schmid CH, Zhang YL, Castro AF, 3rd, Feldman HI, Kusek JW, Eggers P, Van Lente F, Greene T *et al*: **A new equation to estimate glomerular filtration rate.** *Annals of internal medicine* 2009, **150**(9):604-612.
14. Shi H, Jia J, Li D, Wei L, Shang W, Zheng Z: **Blood oxygen level dependent magnetic resonance imaging for detecting pathological patterns in lupus nephritis patients: a preliminary study using a decision tree model.** *BMC nephrology* 2018, **19**(1):33.
15. Park E, Cho M, Ki CS: **Correct use of repeated measures analysis of variance.** *The Korean journal of laboratory medicine* 2009, **29**(1):1-9.
16. Maurissen JP, Vidmar TJ: **Repeated-measure analyses: Which one? A survey of statistical models and recommendations for reporting.** *Neurotoxicology and teratology* 2017, **59**:78-84.
17. Zheng Z, Shi H, Ma H, Li F, Zhang J, Zhang Y: **Renal Oxygenation Characteristics in Healthy Native Kidneys: Assessment with Blood Oxygen Level-Dependent Magnetic Resonance Imaging.** *Nephron Physiology* 2014, **128**(3-4):47-54.
18. Gloviczki ML, Glockner JF, Crane JA, McKusick MA, Misra S, Grande JP, Lerman LO, Textor SC: **Blood oxygen level-dependent magnetic resonance imaging identifies cortical hypoxia in severe renovascular disease.** *Hypertension (Dallas, Tex : 1979)* 2011, **58**(6):1066-1072.
19. Yin WJ, Liu F, Li XM, Yang L, Zhao S, Huang ZX, Huang YQ, Liu RB: **Noninvasive evaluation of renal oxygenation in diabetic nephropathy by BOLD-MRI.** *European journal of radiology* 2012, **81**(7):1426-1431.
20. Xin-Long P, Jing-Xia X, Jian-Yu L, Song W, Xin-Kui T: **A preliminary study of blood-oxygen-level-dependent MRI in patients with chronic kidney disease.** *Magnetic resonance imaging* 2012, **30**(3):330-335.
21. Brezis M, Rosen S: **Hypoxia of the renal medulla—its implications for disease.** *The New England journal of medicine* 1995, **332**(10):647-655.
22. Riggs TE, Shafer AW, Guenter CA: **Acute changes in oxyhemoglobin affinity. Effects on oxygen transport and utilization.** *The Journal of clinical investigation* 1973, **52**(10):2660-2663.

23. Shi H, Yan T, Li D, Jia J, Shang W, Wei L, Zheng Z: **Detection of Renal Hypoxia in Lupus Nephritis Using Blood Oxygen Level-Dependent MR Imaging: A Multiple Correspondence Analysis.** *Kidney & blood pressure research* 2017, **42**(1):123-135.
24. Hansell P, Welch WJ, Blantz RC, Palm F: **Determinants of kidney oxygen consumption and their relationship to tissue oxygen tension in diabetes and hypertension.** *Clinical and experimental pharmacology & physiology* 2013, **40**(2):123-137.
25. Khatir DS, Pedersen M, Jespersen B, Buus NH: **Evaluation of Renal Blood Flow and Oxygenation in CKD Using Magnetic Resonance Imaging.** *American journal of kidney diseases : the official journal of the National Kidney Foundation* 2015, **66**(3):402-411.
26. Ebrahimi B, Gloviczki M, Woollard JR, Crane JA, Textor SC, Lerman LO: **Compartmental analysis of renal BOLD MRI data: introduction and validation.** *Investigative radiology* 2012, **47**(3):175-182.
27. Saad A, Crane J, Glockner JF, Herrmann SM, Friedman H, Ebrahimi B, Lerman LO, Textor SC: **Human renovascular disease: estimating fractional tissue hypoxia to analyze blood oxygen level-dependent MR.** *Radiology* 2013, **268**(3):770-778.

## Figure And Table Legends

**Figure 1:** The way the rectangular ROI was used in the renal R2\* map.

This coronal section of the renal R2\* map came from the left kidney of a patient with LN. The line *AB* linked the renal middle pole and the renal hilus. The line *CD* was connected between the renal upper pole and the lower pole. Point *O* was the junction of the two lines. In order to acquire the consecutive R2\* data along the direction from the superficial cortex to the deep layer medulla, the rectangular ROI was placed in the renal parenchyma BOLD imaging. One tip of the ROI was located on the renal cortical surface. Another tip of the ROI looked out on the point *O*. The long axis of the rectangular ROI is shown by the yellow line.

**Figure 2:** Manifestation of R2\* value from the superficial cortex to the deep medulla.

We detected four samples of R2\* values from one healthy volunteer (A and B) and one patient with LN (C and D). A and C, One pattern of R2\* values manifestation. R2\* values in the superficial cortex fluctuated in a slight magnitude, and we observed only a very small increment of R2\*. However, a remarkable R2\* value augmentation was detected in the deep medullary part. B and D. Another pattern of R2\* values representation in which the R2\* values maintained a stabilized level throughout the depth of the renal parenchyma.

**Figure 3:** Comparison of the tendency of R2\* values between patients with LN and healthy volunteers.

Orange points and green squares indicate  $R2^*$  data for patients with LN and healthy volunteers, respectively. A, Comparison result of  $R2^*$  data in a sharply raising style.  $R2^*$  values of patients with LN are slightly higher than those for healthy volunteers in the cortical zone. The tendency reversed in the deep medullary zone. B, Comparison result of  $R2^*$  data in a slowly raising style.  $R2^*$  values for patients with LN are slightly lower than those of healthy volunteers in the cortical zone. No distinct difference was found in the deep medullary zone.

**Figure 4:** Comparison of the goodness of fit for four mathematic formulas in both the sharply raising style and the slowly raising style of  $R2^*$  data in one patient with LN.

Black dots indicate  $R2^*$  values from the superficial cortical zone to the deep medullary zone. Blue and orange fitted curves are displayed in both the sharply raising style and the slowly raising style of  $R2^*$  data, respectively. Fitted curves from four mathematic functions—Polynomial formula (A and B), formula (C and D), exponential formula (E and F), and Gaussian formula (G and H)—are arranged from top to bottom.

Table 1: Goodness of fit curve parameters in four mathematic functions in the healthy volunteer group

Table 2: Goodness of fit curve parameters in four mathematic functions in the LN group

## Figures

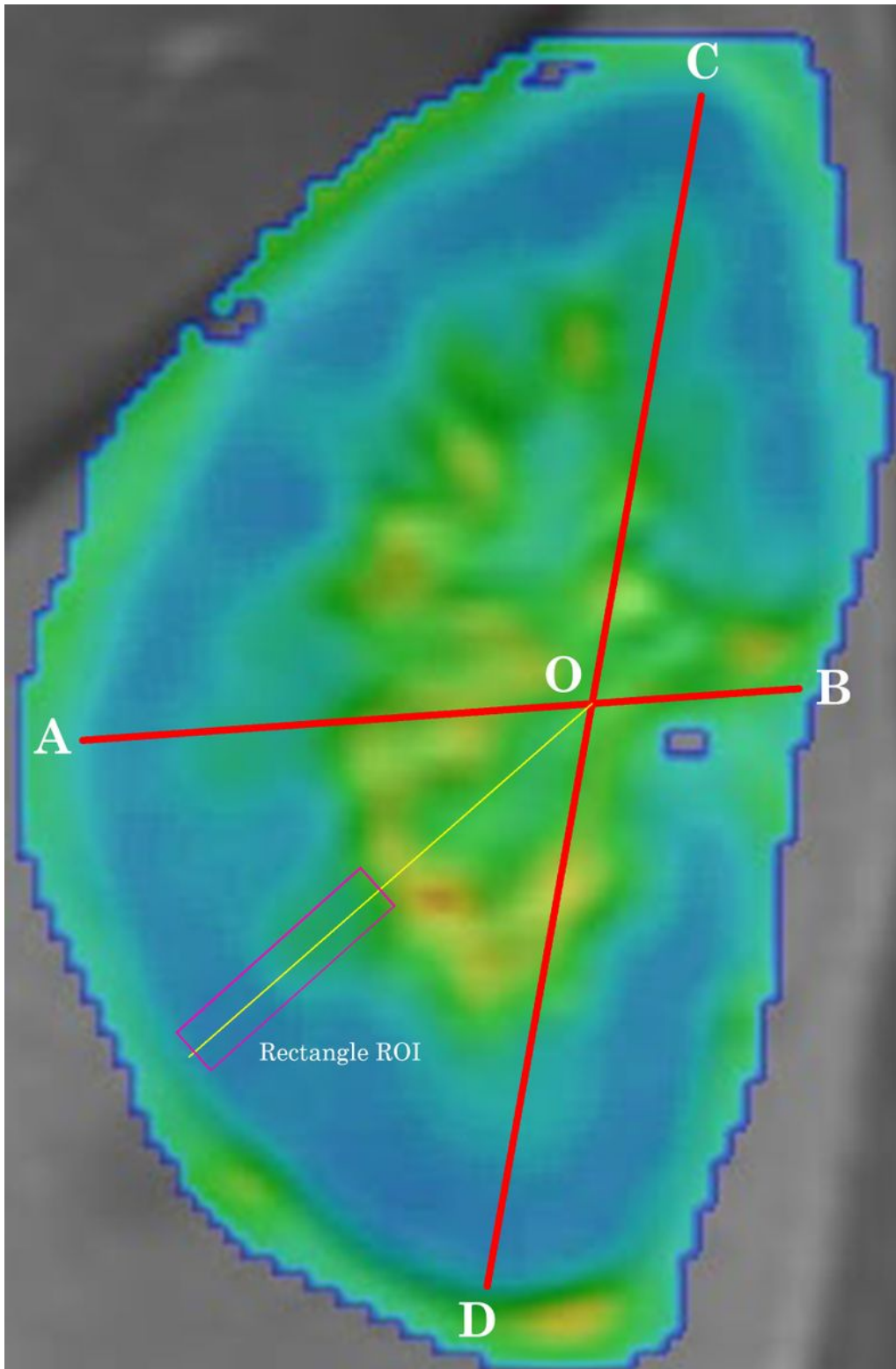


**Figure 1**

The way the rectangular ROI was used in the renal R2\* map. This coronal section of the renal R2\* map came from the left kidney of a patient with LN. The line AB linked the renal middle pole and the renal hilus. The line CD was connected between the renal upper pole and the lower pole. Point O was the junction of the two lines. In order to acquire the consecutive R2\* data along the direction from the superficial cortex to the deep layer medulla, the rectangular ROI was placed in the renal parenchyma

BOLD imaging. One tip of the ROI was located on the renal cortical surface. Another tip of the ROI looked out on the point O. The long axis of the rectangular ROI is shown by the yellow line.

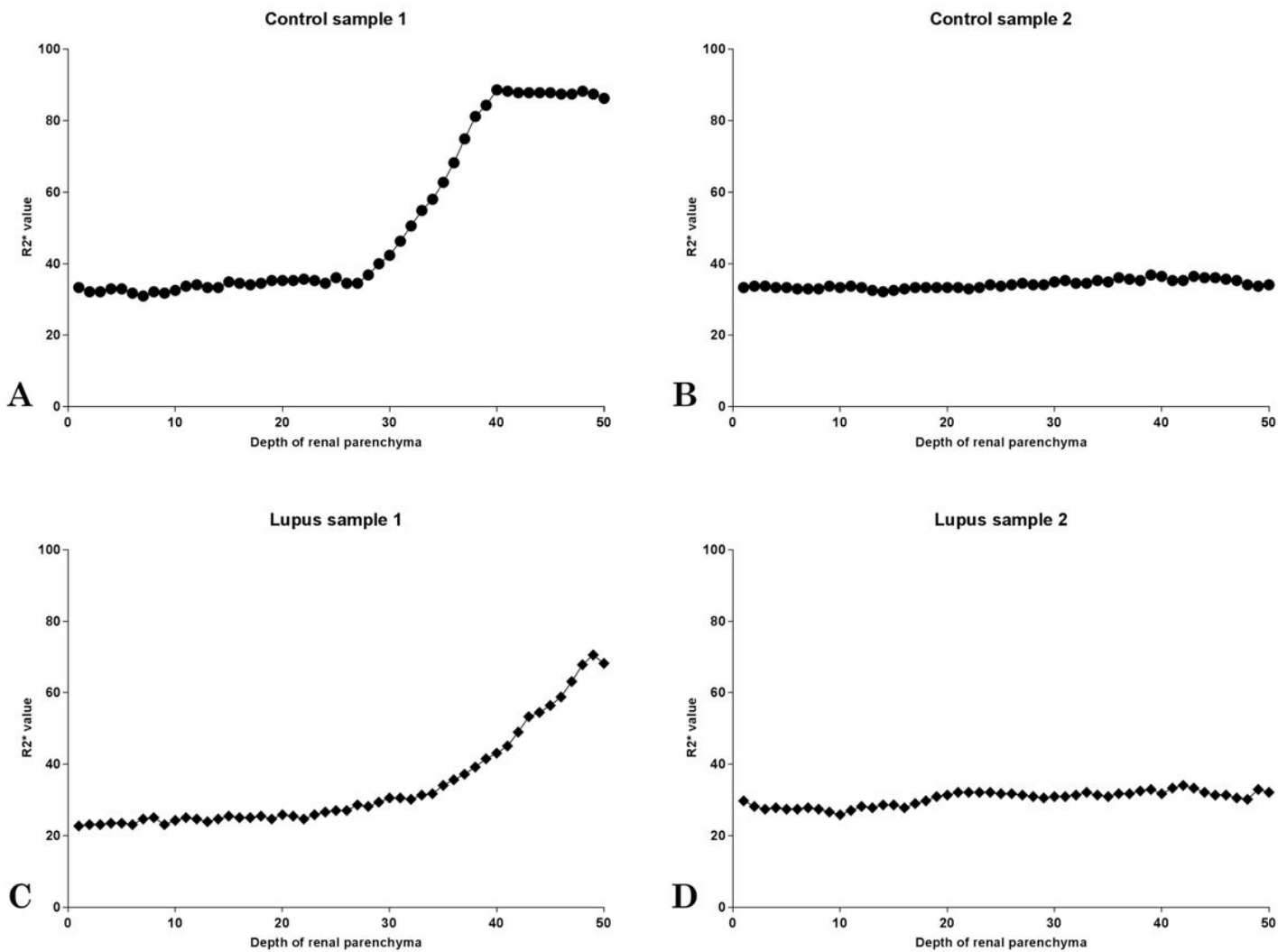


**Figure 2**

Manifestation of R2\* value from the superficial cortex to the deep medulla. We detected four samples of R2\* values from one healthy volunteer (A and B) and one patient with LN (C and D). A and C, One pattern of R2\* values manifestation. R2\* values in the superficial cortex fluctuated in a slight magnitude, and we observed only a very small increment of R2\*. However, a remarkable R2\* value augmentation was detected in the deep medullary part. B and D. Another pattern of R2\* values representation in which the R2\* values maintained a stabilized level throughout the depth of the renal parenchyma.

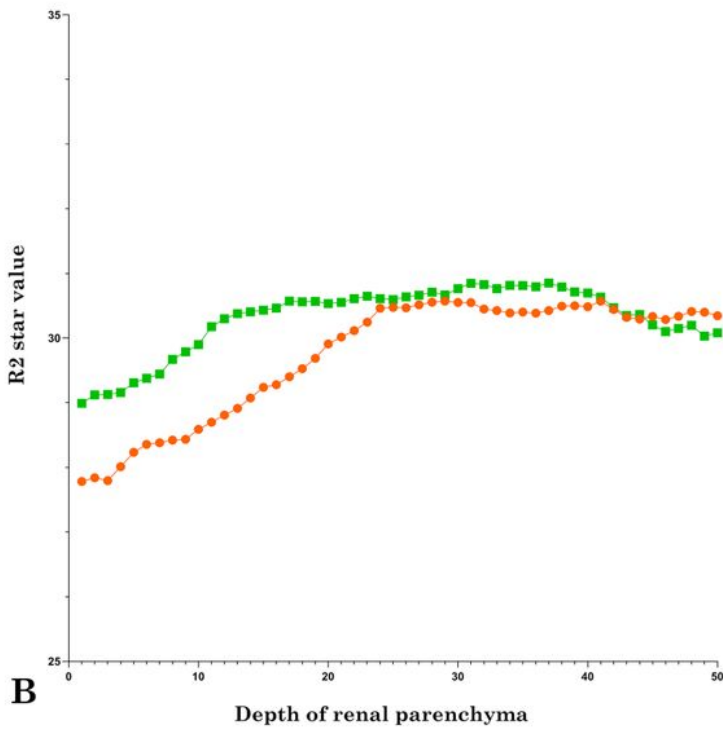
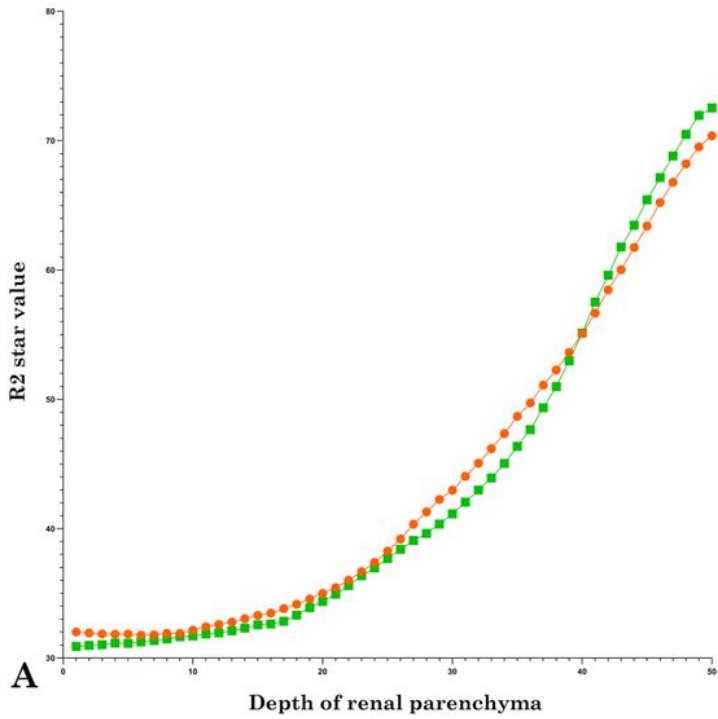


**Figure 3**

Comparison of the tendency of R2\* values between patients with LN and healthy volunteers. Orange points and green squares indicate R2\* data for patients with LN and healthy volunteers, respectively. A, Comparison result of R2\* data in a sharply raising style. R2\* values of patients with LN are slightly higher than those for healthy volunteers in the cortical zone. The tendency reversed in the deep medullary zone. B, Comparison result of R2\* data in a slowly raising style. R2\* values for patients with LN are slightly

lower than those of healthy volunteers in the cortical zone. No distinct difference was found in the deep medullary zone.

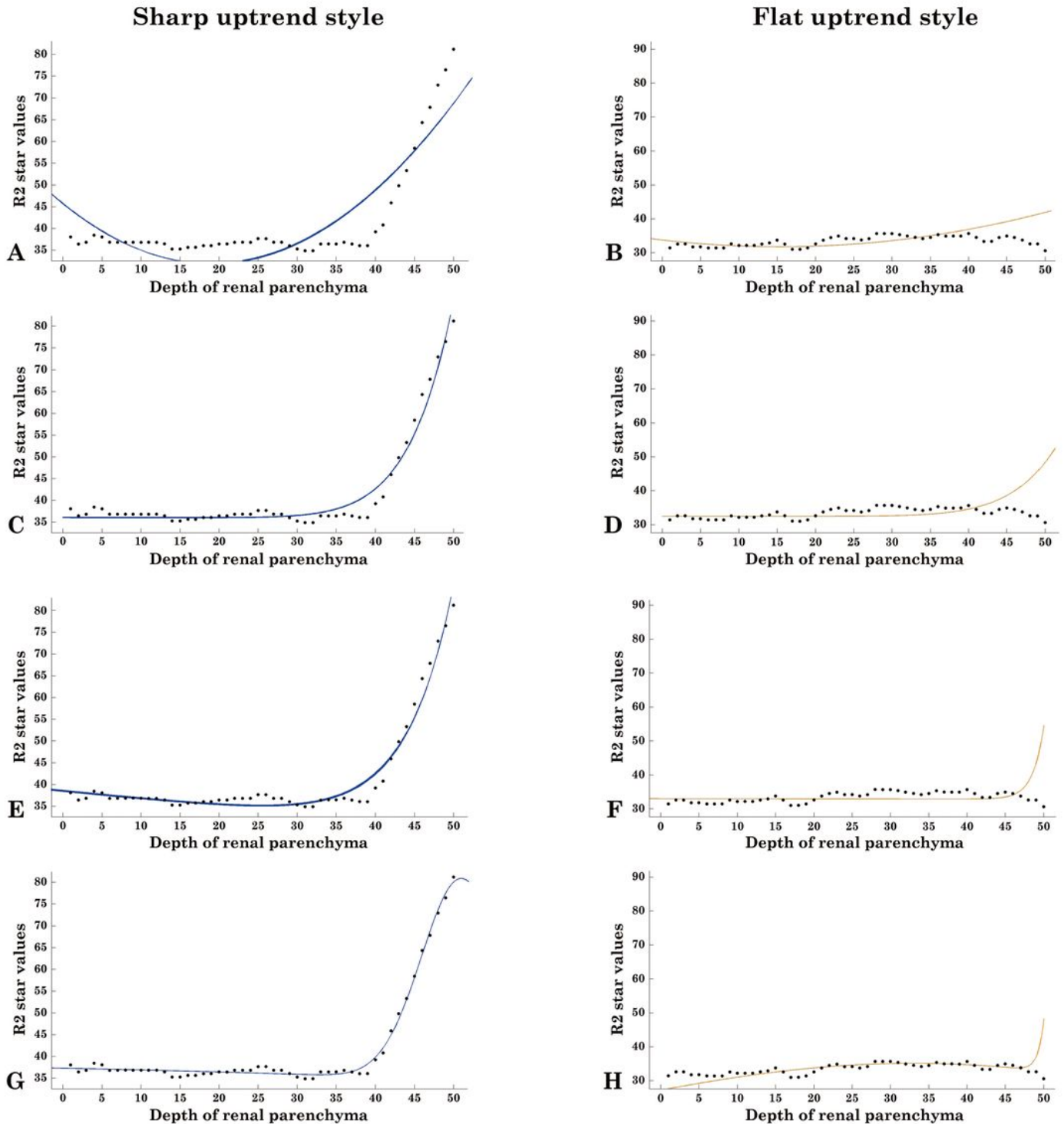


**Figure 4**

Comparison of the goodness of fit for four mathematic formulas in both the sharply raising style and the slowly raising style of  $R2^*$  data in one patient with LN. Black dots indicate  $R2^*$  values from the superficial cortical zone to the deep medullary zone. Blue and orange fitted curves are displayed in both the sharply

raising style and the slowly raising style of  $R^2$  data, respectively. Fitted curves from four mathematic functions—Polynomial formula (A and B), formula (C and D), exponential formula (E and F), and Gaussian formula (G and H)—are arranged from top to bottom.

## Supplementary Files

This is a list of supplementary files associated with this preprint. Click to download.

- [supplement1.pdf](#)